

# ContextFormer: Redefining Efficiency in Semantic Segmentation

Mian Muhammad Naeem Abid, Nancy Mehta, Zongwei Wu, Fayaz Ali Dharejo, Radu Timofte  
Computer Vision Lab, CAIDAS, University of Würzburg, Germany

## Abstract

Semantic segmentation assigns labels to pixels in images, a critical yet challenging task in computer vision. Convolutional methods, although capturing local dependencies well, struggle with long-range relationships. Vision Transformers (ViTs) excel in global context capture but are hindered by high computational demands, especially for high-resolution inputs. Most research optimizes the encoder architecture, leaving the bottleneck underexplored—a key area for enhancing performance and efficiency. We propose ContextFormer, a hybrid framework leveraging the strengths of CNNs and ViTs in the bottleneck to balance efficiency, accuracy, and robustness for real-time semantic segmentation. The framework's efficiency is driven by three synergistic modules: the Token Pyramid Extraction Module (TPEM) for hierarchical multi-scale representation, the **Transformer** and **Modulating DepthwiseConv** (Trans-MDC) block for dynamic scale-aware feature modeling, and the Feature Merging Module (FMM) for robust integration with enhanced spatial and contextual consistency. Extensive experiments on ADE20K, Pascal Context, CityScapes, and COCO-Stuff datasets show ContextFormer significantly outperforms existing models, achieving state-of-the-art mIoU scores, setting a new benchmark for efficiency and performance. The codes will be made publicly available upon acceptance.

## 1. Introduction

Semantic segmentation, a key task in computer vision, assigns each pixel in an image a specific semantic label [45]. Traditional approaches [1, 5, 24, 25, 51] address this challenge by employing stacks of local convolutional kernels to capture long-range spatial dependencies. However, with the advent of Vision Transformers (ViTs), semantic segmentation has undergone a significant transformation [18]. These Transformer-based approaches [7, 62] excel in capturing global context, showcasing superior performance compared to traditional methods. However, their high computational and memory demands pose significant challenges, particularly for real-world applications involving high-resolution

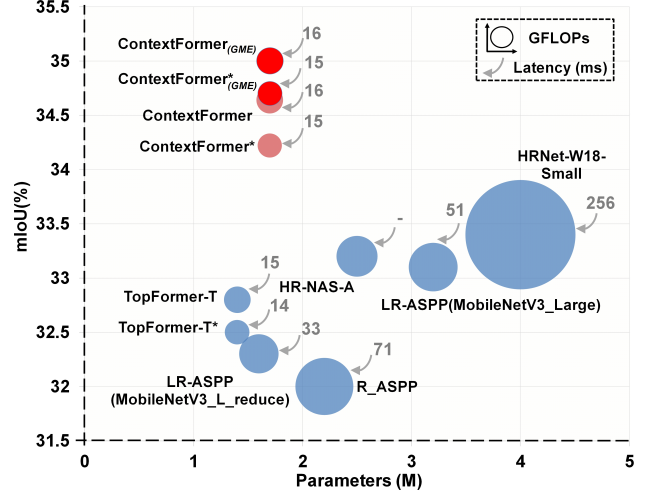


Figure 1. Comparison of mIoU, parameters, GFLOPs, and latency for state-of-the-art efficient models on the ADE20K validation set. Our ContextFormer strikes an optimal balance between performance and efficiency, delivering lower latency while maintaining competitive results. The circle sizes represent GFLOPs, with \* indicating models trained on  $448 \times 448$  input resolution.

input data [11, 36, 39, 42], making them less practical for deployment at scale.

To address this, several efficient strategies, such as local/window-based attention [53], axial attention [26] and lightweight attention mechanisms [36, 37, 43, 48, 69] have been developed. These methods aim to reduce the computational load, but they still struggle to meet the low-latency and the segmentation accuracy essential for real-world applications, especially on high-resolution images (as demonstrated in Fig. 1). To mitigate the computational costs associated with high-resolution processing in a transformer based approach, the authors in [69] applied global attention at a down-scaled resolution of  $1/64$  of the original input, a compromise that inevitably degrades segmentation performance. Conversely, several proposed lightweight Convolutional Neural Networks (CNNs) based models [14, 15, 27, 41, 70] benefit via leveraging asymmetric or depth-wise separable convolutions [28, 52] with linear complexity relative to the input size, making them better

suited for edge device deployment. However, these CNN-based approaches rely on local receptive fields for feature extraction, which constrains their segmentation accuracy.

To further improve the model performance, the researchers explored hybrid transformer-CNN architectures, leveraging the complementary strengths of both paradigms. In TrSeg [30], ResNet serves as the backbone network, while transformer layers are incorporated within the decoder to merge contextual information specific to traffic scenes. Wang *et al.* [61] employed the Swin Transformer [39] to transform an image into a sequence of feature embeddings, utilizing a CNN decoder to reconstruct the spatial dimensions of the feature maps. Several approaches [6, 20, 42, 69] combined them by using CNNs as encoder/backbone for feature extraction and ViTs as bottleneck for improving the efficiency. They had shown improvement in the performance, but at the cost of increased latency. However, despite efforts to balance accuracy, speed, and computational cost, the potential of combining CNNs and ViTs within the bottleneck to synergize long-range and short-range spatial context modeling — offering both performance and efficiency—remains underexplored.

Building on the limitations of prior approaches, we present ContextFormer, a Transformer-based framework for semantic segmentation that efficiently captures both local and global context in the bottleneck design, achieving a balanced trade-off between efficiency, accuracy, and robustness. By integrating three key components—the Token Pyramid Extraction Module (TPEM), **Transformer** and **Modulating DepthwiseConv** (Trans-MDC) block, and **Feature Merging Module** (FMM)—the framework ensures efficient real-time segmentation of high-resolution imagery, delivering high-fidelity predictions tailored for real-world deployment. Specifically, TPEM constructs a hierarchical feature pyramid by fusing image data, gradient magnitude maps, and edge features, leveraging cascaded MobileNetV2 blocks [52] for efficient multi-scale feature extraction with minimal overhead. The Trans-MDC block processes multi-scale tokens from TPEM using a hybrid architecture to dynamically align global dependencies with fine-grained details, producing scale-aware, contextualized features. Complementing this, the FMM establishes robust feature hierarchies through adaptive channel redistribution, enhancing spatial consistency and representational capacity via a gated-shifting mechanism. These enriched features enable ContextFormer to achieve high-fidelity predictions with computational efficiency, optimized for real-world applications.

To rigorously evaluate the efficacy of our proposed approach, we conduct a series of experiments on complex segmentation benchmarks, including ADE20K [73], Pascal Context [46], and CityScapes [9]. To further validate the

generalization of our model, we also apply it to the COCO-Stuff [2] dataset. The primary contributions of the work can be summarized as follows:

- We propose ContextFormer, an innovative framework designed for efficient real-time semantic segmentation.
- We introduce a novel bottleneck design utilizing Trans-MDC blocks, which dynamically capture global dependencies and scale-aware semantics. These blocks, coupled with the TPEM for efficient multi-scale feature extraction and the FMM for adaptive feature integration, ensure robust hierarchical representations essential for dense prediction tasks.
- Our approach achieves state-of-the-art performance on the benchmark datasets, significantly surpassing both mobile-optimized CNN and Transformer-based segmentation models by substantial margins on mIoU.

## 2. Related Work

### 2.1. Efficient Convolutional Neural Networks

Convolutional Neural Networks (CNNs) have dominated computer vision tasks over the last decade, mainly due to their translation equivalence and inductive bias. Recently, researchers have focused on making CNNs more efficient. MobileNet [27, 28, 52], for example, introduced the inverted bottleneck with depth-wise and point-wise convolutions, while ShuffleNet [41, 70] and IGCNet [68] used channel permutation for cross-group information flow. Further efficiency was achieved through models like ENet [49], which reduces resolution early, and GhostNet [23], which optimizes depth-wise convolutions. Models like ERFNet [50] and MobileNeXt [74] enhance speed and feature extraction, while TinyNet [16] and EfficientNet [33, 35] explore scaling parameters to improve performance with less computation. For segmentation, high computational requirements often exceed device capabilities. To address this, DFANet [33] and BiSeNet [64] reduce cost through cross-level aggregation and dual-path architectures, while ICNet [72] and ESPNet [44] use multi-scale input and dilated convolutions. Unlike these approaches, which primarily emphasize local context, our method integrates multi-scale token processing and adaptive feature redistribution, enabling efficient capture of both local and global contextual information.

### 2.2. Lightweight Vision Transformers

Vision Transformers (ViTs) [18] introduced transformer-based architectures to vision, surpassing CNNs in many image recognition tasks. Efforts to stabilize and enhance ViTs involved adding spatial inductive biases [10, 21] and adapting them for broader vision tasks [19, 69] with more efficient self-attention mechanisms [17, 75]. To meet transformers’ data demands, DeiT [57] utilized token-based dis-

tillation, while T2T-ViT [66] reduced token length through token aggregation. Swin Transformer [38] achieved linear complexity by applying self-attention within local windows for greater efficiency. Despite their strong performance, ViTs often have high computational and memory costs, limiting their use on resource-constrained devices [42, 48]. This inspired research into lightweight ViTs, like MobileFormer [6] and MobileViT [42], combining transformer-based self-attention with efficient MobileNet structures. Hybrid models, such as LeViT [20] and EfficientFormer [36], blend CNNs and transformers for enhanced performance-speed balance. RTFormer [60] uses a two-branch architecture based on cross- and GPU-friendly attention. TopFormer [69] incorporates convolutional layers with transformer-based self-attention. These models typically employ a transformer encoder for global context through sequence processing, followed by a transformer or CNN decoder to integrate learned information. However, they often overlook the speed-accuracy tradeoff, leading to high computational demands. In contrast to standard ViT models, the proposed architecture efficiently leverages both CNNs and ViTs by pooling multi-scale tokens as inputs, achieving robust feature learning and improved generalizability.

### 3. Proposed Method

This section presents ContextFormer, an efficient, robust, and powerful segmentation framework that avoids computationally intensive components. As shown in Fig. 2, it is composed of three key modules: (1) a Token Pyramid Encoding Module that captures high-resolution coarse features and low-resolution fine features and generates a feature pyramid, (2) a hybrid Trans-MDC block that efficiently generates scale-aware semantics, and (3) a lightweight Feature Merging Module that fuses these multi-level local and global semantic features to produce semantic segmentation mask via shifted gated mechanism. Next, the details of the model parts are explained below.<sup>1</sup>

#### 3.1. Token Pyramid Encoding Module

Considering the efficiency constraints, the proposed Token Pyramid Encoding module (TPEM) incorporates a series of stacked MobileNet blocks [52], specifically inverted residual blocks. However, unlike MobileNets, the proposed TPEM employs fewer blocks to establish a lightweight hierarchical feature representation. As demonstrated in Fig. 2, an input image  $X \in \mathbb{R}^{5 \times H \times W}$  consists of stacked 3 channel (RGB) image along with the gradient magnitude and edge maps to enhance the semantic richness, where  $H$  and  $W$  are the height and width of the image, respectively. The

<sup>1</sup>For better readability and ease, non-linear activation functions, batch normalization and dropout layers are not mentioned in the equations and figures.

TPEM module initiates by passing this concatenated feature map via a series of MobileNetV2 blocks resulting in multi-scale features  $\{S_1, S_2, \dots, S_L\}$  at different levels, where the number of levels is denoted by  $L$  and the hierarchical feature at each level  $L$  denoted as  $\frac{H}{2^{i+1}} \times \frac{W}{2^{i+1}} \times C_i$ , where  $i \in \{1, 2, 3, 4\}$ . These multi-scale features encompass high-resolution coarse representations alongside low-resolution fine-grained details, which collectively enhance the efficacy of semantic segmentation. To further minimize the computational overhead, an average pooling operation is applied to downsample the extracted tokens to a significantly reduced size, for instance, to  $\frac{1}{64 \times 64}$  of the original input size. Finally, the same sized tokens from different scales are concatenated along the channel dimension to enhance the inter-channel dependencies and produce refined tokens for subsequent blocks. The overall operation of the TPEM is defined as:

$$X_f = \langle S_1^\varphi, S_2^\varphi, S_3^\varphi, S_4^\varphi \rangle \quad (1)$$

Where,  $\varphi$  denotes the average pooling operation applied to the corresponding feature map, and  $\langle . \rangle$  represents the concatenation operation. This combined local feature set is then passed to the Trans-MDC block to extract global and enhanced multi-scale semantics.

#### 3.2. Trans-MDC Block

The average pooled tokens from various scales are unified to a consistent resolution and thereafter concatenated to serve as the input for the Vision Transformer (ViTs) and the Modulating DepthwiseConv block (Trans-MDC). This enables the network to capture a full-image receptive field and extract the rich semantic global and local information in an efficient way. As illustrated in Fig. 2, Trans-MDC block takes as input the combined feature set output of TPEM ( $X_f$ ) and modulates the multi-head attention output of the ViT. Basically, the MDC block draws inspiration from the architectural framework of ViTs, while being composed exclusively of convolutional layers: a  $3 \times 3$  depthwise convolution, a  $1 \times 1$  depthwise convolution, and a  $3 \times 3$  depthwise separable convolution. This design enables the model to learn rich and nuanced features essential for effective semantic segmentation. The inclusion of depthwise convolutions in our design is pivotal due to their significant reduction in computational cost and memory usage. Here, each convolution operation contributes distinct advantages: the  $3 \times 3$  depthwise convolution excels at capturing spatial semantics, while the  $1 \times 1$  depth-wise convolution facilitates the learning of depth-wise cross-channel information. Additionally, the  $3 \times 3$  depth-wise separable convolution integrates both the spatial and channel-wise semantics. Thereafter, the combined semantics,  $\delta'_c$  obtained via aggregating the information from all the three layers are subsequently passed through a channel attention module as

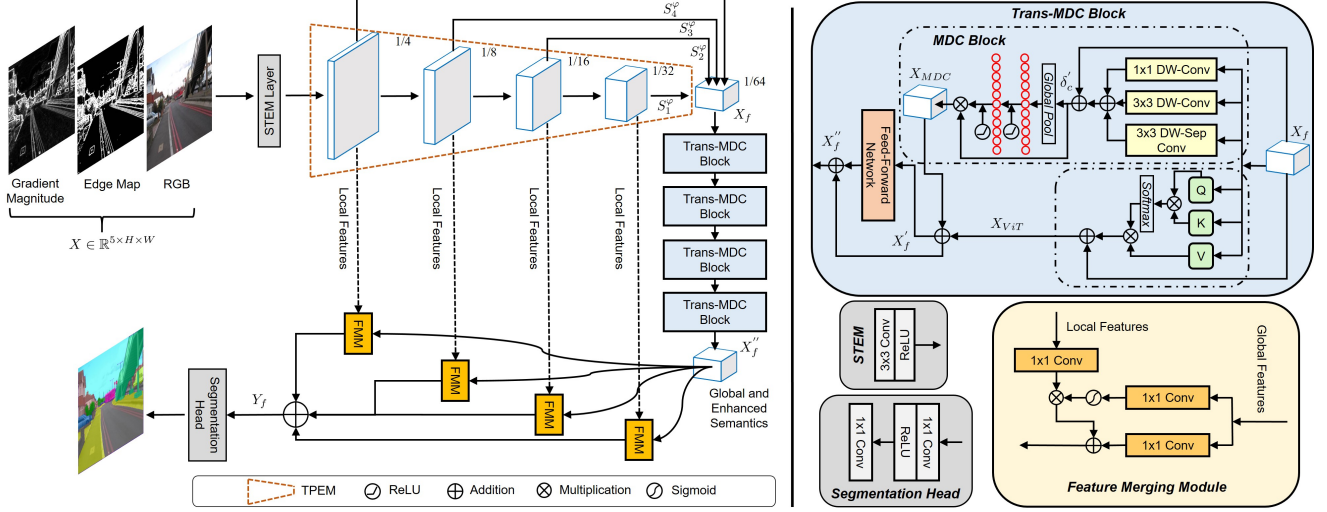


Figure 2. Holistic architecture of the proposed ContextFormer. On (left), the whole architecture is shown, whereas, on (right) details of each of the blocks are depicted.

shown in Eq. (3), which further enhances the global contextual information, thereby boosting the robustness of the extracted features. The overall operation of the MDC block is defined as:

$$\delta'_c = \xi_{3 \times 3}^{dw}(X_f) + \xi_{1 \times 1}^{dw}(X_f) + \xi_{1 \times 1}^{pw}(\xi_{3 \times 3}^{dw}(X_f)) + X_f \quad (2)$$

$$X_{MDC} = \Gamma_2(\Gamma_1(\varphi_g(\delta'_c))) \odot \delta'_c \quad (3)$$

Where,  $\varphi_g$  is the global average pooling layer,  $\Gamma_1$  and  $\Gamma_2$  are two fully-connected layers,  $\odot$  represents the Hadamard product, and  $\xi_{3 \times 3}^{dw}$ ,  $\xi_{1 \times 1}^{dw}$ , and  $\xi_{1 \times 1}^{pw}$  denote  $3 \times 3$  depth-wise,  $1 \times 1$  depth-wise and  $1 \times 1$  point-wise convolution operations, respectively.

Further, as demonstrated in Fig. 2, the ViT block also ingests the pooled feature maps ( $X_f$ ), whereby the global self-attention mechanism facilitates the exchange of information among tokens across the spatial dimension. To maintain the spatial integrity of the tokens and to minimize the frequency of reshaping operations typically associated with ViT architectures, we substitute the conventional linear layers with  $1 \times 1$  convolutional layers. In our implementation of multi-head attention within the ViT framework, we configure the dimensions for the  $Q, K, V$  representations to be 16, 16, and 32, respectively. This dimensional reduction serves to further decrease the overall computational complexity of the model. Additionally, we opt for batch normalization over layer normalization for faster inference. It is important to note that batch normalization is applied following each convolutional layer throughout the network, with the exception of the final output convolution layer. Furthermore, we replace the GELU non-linear activation function originally employed in ViT with ReLU6 [28]

in our architecture, thereby enhancing performance while retaining effective activation characteristics.

$$X_{ViT} = \text{Attention}(X_f) + X_f \quad (4)$$

Where,  $\text{Attention} = \text{softmax}\left(\frac{QK^T}{\sqrt{d_k}}\right)V$ . Finally, the output features from both the blocks are combined to achieve efficient and enhanced features.

$$X'_f = X_{ViT} + X_{MDC} \quad (5)$$

The unified output semantics from the Trans-MDC block are thereby passed through the feed-forward network. For the feed-forward network, following [29, 65], we have integrated depth-wise convolution layer between  $1 \times 1$  convolution layers and to further minimize the computational complexity, expansion factor of two is incorporated which helps the Trans-MDC block to augment the capturing of global semantics. The architectural details about FFN are given in the supplementary. The overall operation of Trans-MDC block can be summarized as follows:

$$X''_f = \text{FFN}(X'_f) + X'_f \quad (6)$$

### 3.3. Feature Merging Module and Segmentation Head

After obtaining robust and enhanced semantics from the Trans-MDC block, Feature Merging Module (FMM) is incorporated to merge the complementary features from the Token Pyramid Encoding Module (TPEM) and Trans-MDC block. FMM module tries to alleviate the semantic gap of the different incoming information and allows the model to have both the local and global context information via its



gated shifted mechanism. To this end, in FMM, firstly the local features from TPME are passed through a  $1 \times 1$  convolution layer. Further, to get a weight matrix for the global features, a  $1 \times 1$  convolution layer followed by Sigmoid activation function is applied on the global features/semantics from Trans-MDC block. Subsequently, the global semantics are integrated into the local tokens via the Hadamard product, and these global semantics are further summed, as shown in Fig. 2, with the local features via a  $1 \times 1$  convolution layer to focus on the relevant semantics. The overall operation of FMM module is summarized as follows:

$$Y_f = (\xi_{1 \times 1}^{c1}(X_f)) \odot (\sigma(\xi_{1 \times 1}^{c2}(X_f''))) + \xi_{1 \times 1}^{c3}(X_f'') \quad (7)$$

Where, the first term before the Hadamard product denotes the processing on the local tokens incoming from the TPME module, the second term denotes the gated operation being performed on the features from the Trans-MDC block to obtain a weight matrix, and  $\sigma$  denotes Sigmoid activation function.

After obtaining enhanced features from the FMM, low-resolution features are upsampled to match the high-resolution features and summed element-wise. The resulting features are then passed through the Segmentation Head, comprising of two  $1 \times 1$  convolution layers, to generate the final segmentation map.

## 4. Experiments

### 4.1. Datasets and Measures

We conduct the experiments on four benchmark datasets: ADE20K [73], PASCAL Context [46], CityScapes [9] and COCO-Stuff [2]. In total, **ADE20K** [73] dataset consists of 25000 images, containing 150 class categories. The division of dataset is as follows: 20000 images for training, 2000 images for validation and 3000 images for testing. The **PASCAL Context** [46] dataset contains 1 background, and 59 semantic labels. Out of 10103 images in total, training and testing scene images are split into 4998 and 5105, respectively. The **CityScapes** [9] dataset consists of 19 fine class annotations. 2975 images are taken into account for training and 500 images for validation/testing. Pixel-level stuff annotations were applied on COCO dataset for augmentation, resulting in **COCO-Stuff** [2] dataset. From COCO dataset, 10000 images are picked, where 9000 images are considered for training and 1000 images for testing.

Following the recent literature [3, 31, 69] we report the results using the standard common measures: Mean Intersection over Union (mIoU) for segmentation accuracy, Giga Floating Point Operations per Second (GFLOPs), latency and number of parameters.

### 4.2. Implementation Details

Our implementation is based on PyTorch and MMSegmentation toolbox [8]. All the models are first pretrained on ImageNet-1K dataset [12], including our proposed ContextFormer<sup>2</sup> model. Further, they are fined-tuned on semantic segmentation datasets. Batch-Normalization layers are used after almost each convolution layer except the last output layer. For the **ADE20K** dataset, we follow data augmentations same as in [62] for fair comparison. Moreover, for ADE20K dataset, we use batch size 16, and 160K scheduler by following [62] and [69]. Various augmentations have been applied such as random scaling, random cropping, random horizontal flip, random resize etc. For the **CityScapes** dataset, same data augmentations are followed as in [62, 69]. Images are resized and rescaled with same crop size *i.e.*  $1024 \times 512$ . It should be noted that for all datasets and models, we set  $1.2 \times 10^{-4}$  as the initial learning rate with the weight decay set to 0.01. However, initial learning rate for the CityScapes dataset is set to  $3 \times 10^{-4}$ . For the **PASCAL Context** and **COCO-Stuff** datasets, 80K training iterations are implemented. Additionally, for both datasets, same data augmentations and training settings are incorporated as in [8] and the training images are resized and cropped to  $512 \times 512$  and  $480 \times 480$  for COCO-Stuff and PASCAL Context datasets, respectively.

### 4.3. Experiments on ADE20K

As illustrated in Tab. 1, the proposed model is compared with the state-of-the-art approaches, consisting of efficient CNNs [25, 27, 52, 55] and lightweight ViTs [13, 32, 41, 62, 69], on the validation set of ADE20K dataset. For performance and efficiency evaluation, mIoU, GFLOPs, parameters, and latency are taken into account. The proposed model is trained for the following input resolutions:  $512 \times 512$  and  $448 \times 448$  on ADE20K dataset.

DeepLabV3+ with MobileNetV2 as encoder achieved best mIoU *i.e.* 38.1%. Notwithstanding, it encompasses a substantially higher computational burden measured in GFLOPs, latency contrasting with the proposed model, which achieves comparable efficacy with 25.2 less GFLOPs—representing a reduction of 97.67%—and 13.7M (88.96%) fewer parameters while just having 16ms latency, signifying a decrease in complexity.

Among the CNN-based baselines, the most popular model utilizing MobileNetV3-Large [27] as the encoder and LR-ASPP as the decoder strikes an effective balance between the computational complexity (2.0 GFLOPs, 51 ms latency) and accuracy (33.1% mIoU). Towards the effort to make this model more efficient, a reduced version, called MobileNetV3-Large-reduce by decreasing the number of feature maps of the model was used. Our proposed

<sup>2</sup>On ImageNet-1K dataset, ContextFormer achieves 66.11% Top-1 accuracy. Details are provided in the supplementary material.

Table 1. Quantitative results of various models on ADE20K *validation* set [73]. \* indicates results from models trained with  $448 \times 448$  input size. For fair comparison with SegFormer and TopFormer, batch size of 16 is considered for ContextFormer. Whereas, batch size of 32 is considered for CNN based models. GFLOPs are reported for input resolution of  $512 \times 512$ . Single-scale inference is used to report mIoU. ‘-’ means the unreported results, and ContextFormer<sub>(GME)</sub> is proposed model with concatenated edge and magnitude maps.

Models	Encoder	mIoU	GFLOPs	Parameters	Latency(ms)
PSPNet [71]	MobileNetV2 [52]	29.6	52.2	13.7M	426
FCN-8s [40]	MobileNetV2 [52]	19.7	39.6	9.8M	406
Semantic FPN [32]	ConvMLP-S [34]	35.8	33.8	12.8M	311
DeepLabV3+ [4]	EfficientNet [56]	36.2	26.9	17.1M	388
DeepLabV3+ [4]	MobileNetV2 [52]	38.1	25.8	15.4M	414
Lite-ASPP [4]	ResNet18 [25]	37.5	19.2	12.5M	259
DeepLabV3+ [4]	ShuffleNetv2-1.5x [41]	37.6	15.3	16.9M	384
HRNet-Small [67]	HRNet-W18-Small [67]	33.4	10.2	4.0M	256
SegFormer [62]	MiT-B0 [62]	37.4	8.4	3.8M	308
Lite-ASPP [4]	MobileNetV2 [52]	36.6	4.4	2.9M	94
R-ASPP [52]	MobileNetV2 [52]	32.0	2.8	2.2M	71
HR-NAS-B [13]	Searched [13]	34.9	2.2	3.9M	-
LR-ASPP [27]	MobileNetV3-Large [27]	33.1	2.0	3.2M	51
HR-NAS-A [13]	Searched [13]	33.2	1.4	2.5M	-
LR-ASPP [27]	MobileNetV3-Large-reduce [27]	32.3	1.3	1.6M	33
TopFormer* [69]	TopFormer-T [69]	32.5	0.5	1.4M	14
TopFormer [69]	TopFormer-T [69]	32.8	0.6	1.4M	15
ContextFormer* (Ours)	TPEM	34.2	0.5	1.7M	15
ContextFormer (Ours)	TPEM	34.6	0.6	1.7M	16
ContextFormer* <sub>(GME)</sub> (Ours)	TPEM	34.7	0.5	1.7M	15
ContextFormer <sub>(GME)</sub> (Ours)	TPEM	35.0	0.6	1.7M	16

Table 2. Comparison of ContextFormer with more *recent efficient models* on ADE20K dataset [73]. \* indicates results from models trained with  $448 \times 448$  input size.

Models	Encoder	mIoU	GFLOPs	Parameters
PEM [3]	STDC1 [3]	39.6	16.0	17.0M
FeedFormer-B0 [54]	MiT-B0 [62]	39.2	7.8	4.5M
SegNeXt [22]	SegNeXt-T [22]	41.1	6.6	4.3M
U-MixFormer [63]	MiT-B0 [62]	41.2	6.1	6.1M
MegaSeg [31]	MegaSeg-T [31]	42.4	5.5	4.7M
CGRSeg [47]	CGRSeg-T [47]	43.6	4.0	9.4M
RepViT [58]	RepViT-M1.1 [58]	40.6	-	-
TopFormer* [69]	TopFormer-T [69]	32.5	0.5	1.4M
TopFormer [69]	TopFormer-T [69]	32.8	0.6	1.4M
ContextFormer* (Ours)	TPEM	34.2	0.5	1.7M
ContextFormer (Ours)	TPEM	34.6	0.6	1.7M
ContextFormer* <sub>(GME)</sub> (Ours)	TPEM	34.7	0.5	1.7M
ContextFormer <sub>(GME)</sub> (Ours)	TPEM	35.0	0.6	1.7M

ContextFormer (35.0% mIoU) surpasses both the LR-ASPP models in accuracy by 1.9% and 2.7% respectively, while having much lower latency (16ms), thus proving its robustness. This represents a latency reduction of 68.63% compared to LR-ASPP and 51.52% compared to LR-ASPP reduce. In ViT-based models, HR-NAS-B [13] integrates Transformer blocks into the HRNet [59] architecture using neural architecture search, achieving an effective balance

between computational complexity (2.2 GFLOPs) and accuracy (34.9% mIoU). SegFormer has shown good performance of 37.4% mIoU. Nevertheless, the proposed model achieves mIoU of 35.0% while having 92.9% and 2.1M (56.4%) fewer GFLOPs and parameters, respectively compared to SegFormer, and 0.1% higher mIoU than HR-NAS-B. Moreover, ContextFormer demonstrates a 72.7% reduction in GFLOPs compared to HR-NAS-B and a 92.9% reduction compared to SegFormer. The superior performance of ContextFormer can be attributed to the incorporation of a robust bottleneck Trans-MDC block, which synergistically leverages the strengths of both ViT and CNNs. This design facilitates the efficient extraction and representation of robust features, optimizing the trade-off between computational efficiency and model expressiveness. It is worth emphasizing that the integration of edge maps enhances performance, as evidenced by improved mIoU metric.

For further demonstrating the effectiveness of the proposed ContextFormer, we also report the results on some recent SOTA semantic segmentation approaches in different settings. It can be clearly seen in Tab. 2 that unlike other approaches, it achieves better trade-off between performance and efficiency.



Figure 3. Visual results on the ADE20K validation set. The results highlight the proposed model’s effectiveness in producing high-quality segmentation maps with improved spatial consistency.

#### 4.3.1. Visual Results

Fig. 3 illustrates the qualitative results of our proposed model, compared alongside the original images, ground truth annotations, and the segmentation results produced by TopFormer [69]. The input images used for this evaluation are sourced from the validation set of the ADE20K benchmark dataset, which is renowned for its challenging and diverse scenes. A detailed examination of the visual outputs reveals that our model consistently delivers more precise segmentation results, capturing finer details and producing more realistic predictions compared to TopFormer. These improvements are particularly evident in regions with intricate boundaries and small objects, where TopFormer often exhibits over-smoothing or segmentation errors. The superior performance of both of our models underscores its robustness and ability to effectively learn and generalize complex visual features from the dataset. Such results not only demonstrate the model’s capacity for capturing subtle details but also highlight its potential for real-world applications requiring high-quality semantic segmentation with improved edge fidelity and accuracy.

#### 4.3.2. Ablation Study

As elaborated in Tab. 3, we analyze the contribution of the Trans-MDC block to the overall performance of the model, focusing on its individual components and their collective impact. The study is divided into two parts, examining the **Modulating DepthwiseConv (MDC)** block’s architecture and the integration of Vision Transformer (ViT) components.

**Effects of MDC Block Design:** The upper half of the study highlights the incremental benefits of specific design

Table 3. Ablation studies of ContextFormer on the ADE20K validation set [73].

ViT <sub>block</sub>	ContextFormer (Trans-MDC)					mIoU	GFLOPs	Parameters
	$3 \times 3_{dw}$	$1 \times 1_{dw}$	$3 \times 3_{dw,sep}$	C-Attn	GME			
	✓					25.4	0.55	1.02M
	✓	✓				25.6	0.55	1.10M
	✓		✓			28.7	0.56	1.29M
	✓	✓	✓	✓		29.5	0.56	1.38M
	✓		✓		✓	29.8	0.56	1.38M
✓						32.7	0.54	1.41M
✓	✓					32.8	0.57	1.42M
✓	✓	✓				32.9	0.57	1.43M
✓	✓	✓	✓			33.8	0.58	1.61M
✓	✓		✓	✓		34.6	0.58	1.68M
✓	✓	✓	✓	✓	✓	35.0	0.58	1.68M

choices within the MDC block. Starting with the baseline configuration, which includes a  $3 \times 3$  depth-wise convolution layer, we observe that augmenting it with an additional  $1 \times 1$  depth-wise convolution layer enhances the model’s segmentation accuracy by 0.2%. This improvement, though marginal, demonstrates the effectiveness of fine-grained feature extraction at multiple scales. The inclusion of a third parallel branch in the MDC block, comprising a  $3 \times 3$  depth-wise separable convolution, significantly boosts performance by 3.3%. This substantial improvement underscores the importance of capturing spatial hierarchies and multi-scale contextual information for robust feature representation, thus capturing the global dependencies. Additionally, the integration of a channel attention layer further refines the extracted features, albeit with a smaller but meaningful performance gain, highlighting its utility in emphasizing critical feature channels.

**Effect of Trans-MDC Block and GME Map:** In the lower half of the study, we evaluate the synergy between the ViT backbone and the proposed MDC block. Initially, the model demonstrates a substantial 32.7% mIoU improvement when utilizing ViT alone, even without the MDC block, validating ViT’s efficacy in enhancing semantic feature representation. However, the stepwise inclusion of depth-wise convolution layers from the MDC block markedly improves the model’s performance. The addition of each MDC component further strengthens ViT’s capability to capture local and global context, resulting in a cumulative performance improvement of approximately 2%, as detailed. These results provide compelling evidence that the MDC block not only complements ViT but also enhances its effectiveness, resulting in a robust architecture that excels in overall segmentation tasks. Furthermore, the inclusion of edge maps alongside the RGB image further amplifies the model’s performance by 0.4%, thus effectively capturing sharp and fine-grained features within the image. This proves that the edge maps act as a complementary input, guiding the segmentation process by emphasizing object boundaries and delineating intricate structures.

Table 4. Results on PASCAL Context *test* set [46].

Methods	Backbone	mIoU <sup>59</sup>	mIoU <sup>60</sup>	GFLOPs
DeepLabV3+ [4]	ENet-s16 [49]	43.07	39.19	23.00
DeepLabV3+ [4]	MobileNetV2-s16 [52]	42.34	38.59	22.24
LR-ASPP [27]	MobileNetV3-s16 [27]	38.02	35.05	2.04
TopFormer [69]	TopFormer-T [69]	40.39	36.41	0.53
ContextFormer (Ours)	TPEM	41.84	37.49	0.47
ContextFormer <sub>(GME)</sub> (Ours)	TPEM	41.85	37.78	0.49

#### 4.4. Results on PASCAL Context

Tab. 4 highlights the comparative performance on the PASCAL Context dataset for 59-class and 60-class configurations. DeepLabV3+ with ENet-s16 and MobileNetV3-s16 backbones achieves mIoU<sup>59</sup>/mIoU<sup>60</sup> scores of 43.07%/39.19% and 42.34%/38.59%, respectively, but with high computational costs of 23.00 and 22.24 GFLOPs. In contrast, the proposed model delivers competitive mIoU<sup>59</sup>/mIoU<sup>60</sup> scores of 41.85%/37.78%, with 22.51 (97.87%) fewer GFLOPs, showcasing its efficiency.

LR-ASPP achieves mIoU<sup>59</sup>/mIoU<sup>60</sup> scores of 38.02%/35.05% using only 2.04 GFLOPs, but our model surpasses it by 3.83%/2.73% with a marginal reduction of 1.55 (75.98%) GFLOPs. Similarly, TopFormer balances performance and efficiency but is outperformed by our model, which achieves 1.46% and 1.37% higher mIoU<sup>59</sup> and mIoU<sup>60</sup>, respectively, while reducing GFLOPs by 0.04 (7.55%). These results establish the proposed model as achieving the optimal trade-off between performance and computational efficiency.

#### 4.5. Results on CityScapes

To further validate the efficacy of the proposed method, we summarize the results on the CityScapes dataset in Tab. 5. While PSPNet and FCN, both with MobileNetV2 encoders, achieve high accuracy, they demand 423.4 and 317.1 GFLOPs, respectively. In comparison, our model achieves 6.5% higher mIoU than FCN with a 315.9 (99.62%) GFLOPs reduction and delivers performance comparable to PSPNet with 422.2 (99.71%) fewer GFLOPs.

L-ASPP achieves the best performance among CNN-based models but at the cost of 11.4 (90.5%) additional GFLOPs. Similarly, SegFormer, a ViT-based model, achieves 71.9% mIoU but requires 17.7 GFLOPs, whereas our method matches its performance with 16.5 (93.22%) fewer GFLOPs. Additionally, our model also surpasses TopFormer with 1.5% higher mIoU at the same computational cost, demonstrating a superior balance of performance and efficiency.

#### 4.6. Results on COCO-Stuff

Tab. 6 summarizes the performance of various models on the COCO-Stuff dataset. While DeepLabV3+ with EfficientNet-s16 achieves the highest mIoU, it incurs a sub-

Table 5. Results on CityScapes *validation* set [9].

Methods	Encoder	mIoU	GFLOPs
PSPNet [71]	MobileNetV2 [52]	70.2	423.4
FCN [40]	MobileNetV2 [52]	61.5	317.1
SegFormer [62]	MiT-B0 [62]	71.9	17.7
L-ASPP [4]	MobileNetV2 [52]	72.7	12.6
LR-ASPP [27]	MobileNetV3-Large [27]	72.4	9.7
LR-ASPP [27]	MobileNetV3-Small [27]	68.4	2.9
TopFormer [69]	TopFormer-T [69]	66.5	1.2
ContextFormer (Ours)	TPEM	68.0	1.2
ContextFormer <sub>(GME)</sub> (Ours)	TPEM	68.0	1.2

Table 6. Results on COCO-Stuff *test* set [2].

Methods	Encoder	mIoU	GFLOPs
PSPNet [71]	MobileNetV2-s8 [52]	30.14	52.94
DeepLabV3+ [4]	EfficientNet-s16 [56]	31.45	27.10
DeepLabV3+ [4]	MobileNetV2-s16 [52]	29.88	25.90
LR-ASPP [27]	MobileNetV3-s16 [27]	25.16	2.37
TopFormer [69]	TopFormer-T [69]	28.34	0.64
ContextFormer (Ours)	TPEM	29.00	0.58
ContextFormer <sub>(GME)</sub> (Ours)	TPEM	29.12	0.6

stantial computational cost. In contrast, the proposed model achieves comparable accuracy with 26.50 (97.8%) fewer GFLOPs, demonstrating its computational efficiency. Similarly, compared to DeepLabV3+ with MobileNetV2-s16, which consumes 25.90 GFLOPs for an mIoU of 29.88%, our model achieves similar performance with 25.30 (97.7%) fewer GFLOPs, highlighting its scalability. Additionally, our method matches PSPNet’s accuracy while significantly reducing computational demand and surpasses TopFormer with a 0.78% higher mIoU and 0.04 (6.25%) fewer GFLOPs. These results establish the proposed model as a robust and efficient solution, achieving an optimal balance between performance and computational cost for real-world applications.

## 5. Conclusion

In this paper, we propose a hybrid architecture called ContextFormer, for the complex problem of semantic segmentation. ContextFormer takes into account the advantages of both ViT and CNN, specifically in the bottleneck part of the model. The whole pipeline is based on efficient choices. Extensive experiments on four benchmark datasets reveal that ContextFormer finds a better trade-off between performance and efficiency than the prior works. The general nature of the model makes it suitable to be added to various other methods to improve performance and efficiency. In future, the proposed method will be tested across a range of numerous other domains. Moreover, it can serve as a baseline for future research in the direction of efficient models that combine ViTs and CNNs.



## References

- [1] Vijay Badrinarayanan, Alex Kendall, and Roberto Cipolla. Segnet: A deep convolutional encoder-decoder architecture for image segmentation. *IEEE transactions on pattern analysis and machine intelligence*, 39(12):2481–2495, 2017. 1
- [2] Holger Caesar, Jasper Uijlings, and Vittorio Ferrari. Coco-stuff: Thing and stuff classes in context. In *Proceedings of the IEEE conference on computer vision and pattern recognition*, pages 1209–1218, 2018. 2, 5, 8
- [3] Niccolò Cavagnero, Gabriele Rosi, Claudia Cuttano, Francesca Pistilli, Marco Ciccone, Giuseppe Averta, and Fabio Cermelli. Pem: Prototype-based efficient maskformer for image segmentation. In *Proceedings of the IEEE/CVF Conference on Computer Vision and Pattern Recognition*, pages 15804–15813, 2024. 5, 6
- [4] Liang-Chieh Chen, Yukun Zhu, George Papandreou, Florian Schroff, and Hartwig Adam. Encoder-decoder with atrous separable convolution for semantic image segmentation. In *Proceedings of the European conference on computer vision (ECCV)*, pages 801–818, 2018. 6, 8
- [5] Liang-Chieh CHEN, Yukun ZHU, George PAPANDREOU, F Schroff, Aug CV, and H Adam. Deeplabv3+: Encoder-decoder with atrous separable convolution for semantic image segmentation [m]. ferrari v, hebert m, sminchisescu c, et al. eccv (7), 2018. 1
- [6] Yinpeng Chen, Xiyang Dai, Dongdong Chen, Mengchen Liu, Xiaoyi Dong, Lu Yuan, and Zicheng Liu. Mobileformer: Bridging mobilenet and transformer. In *Proceedings of the IEEE/CVF conference on computer vision and pattern recognition*, pages 5270–5279, 2022. 2, 3
- [7] Bowen Cheng, Ishan Misra, Alexander G Schwing, Alexander Kirillov, and Rohit Girdhar. Masked-attention mask transformer for universal image segmentation. In *Proceedings of the IEEE/CVF conference on computer vision and pattern recognition*, pages 1290–1299, 2022. 1
- [8] MMSegmentation Contributors. MMSegmentation: Openmmlab semantic segmentation toolbox and benchmark. <https://github.com/open-mmlab/mms Segmentation>, 2020. 5
- [9] Marius Cordts, Mohamed Omran, Sebastian Ramos, Timo Rehfeld, Markus Enzweiler, Rodrigo Benenson, Uwe Franke, Stefan Roth, and Bernt Schiele. The cityscapes dataset for semantic urban scene understanding. In *Proceedings of the IEEE conference on computer vision and pattern recognition*, pages 3213–3223, 2016. 2, 5, 8
- [10] Zihang Dai, Hanxiao Liu, Quoc V Le, and Mingxing Tan. Coatnet: Marrying convolution and attention for all data sizes. *Advances in neural information processing systems*, 34:3965–3977, 2021. 2
- [11] Mostafa Dehghani, Josip Djolonga, Basil Mustafa, Piotr Padlewski, Jonathan Heek, Justin Gilmer, Andreas Peter Steiner, Mathilde Caron, Robert Geirhos, Ibrahim Alabdulmohsin, et al. Scaling vision transformers to 22 billion parameters. In *International Conference on Machine Learning*, pages 7480–7512. PMLR, 2023. 1
- [12] Jia Deng, Wei Dong, Richard Socher, Li-Jia Li, Kai Li, and Li Fei-Fei. Imagenet: A large-scale hierarchical image database. In *2009 IEEE conference on computer vision and pattern recognition*, pages 248–255. Ieee, 2009. 5
- [13] Mingyu Ding, Xiaochen Lian, Linjie Yang, Peng Wang, Xiaojie Jin, Zhiwu Lu, and Ping Luo. Hr-nas: Searching efficient high-resolution neural architectures with lightweight transformers. In *Proceedings of the IEEE/CVF conference on computer vision and pattern recognition*, pages 2982–2992, 2021. 5, 6
- [14] Xiaohan Ding, Yuchen Guo, Guiguang Ding, and Jungong Han. Acnet: Strengthening the kernel skeletons for powerful cnn via asymmetric convolution blocks. In *Proceedings of the IEEE/CVF international conference on computer vision*, pages 1911–1920, 2019. 1
- [15] Xiaohan Ding, Xiangyu Zhang, Ningning Ma, Jungong Han, Guiguang Ding, and Jian Sun. Repvgg: Making vgg-style convnets great again. In *Proceedings of the IEEE/CVF conference on computer vision and pattern recognition*, pages 13733–13742, 2021. 1
- [16] Wei Dong, Jiamei Lv, Gonglong Chen, Yihui Wang, Huikang Li, Yi Gao, and Dinesh Bharadia. TinyNet: A lightweight, modular, and unified network architecture for the internet of things. In *Proceedings of the 20th Annual International Conference on Mobile Systems, Applications and Services*, pages 248–260, 2022. 2
- [17] Xiaoyi Dong, Jianmin Bao, Dongdong Chen, Weiming Zhang, Nenghai Yu, Lu Yuan, Dong Chen, and Baining Guo. Cswin transformer: A general vision transformer backbone with cross-shaped windows. In *Proceedings of the IEEE/CVF conference on computer vision and pattern recognition*, pages 12124–12134, 2022. 2
- [18] Alexey Dosovitskiy, Lucas Beyer, Alexander Kolesnikov, Dirk Weissenborn, Xiaohua Zhai, Thomas Unterthiner, Mostafa Dehghani, Matthias Minderer, Georg Heigold, Sylvain Gelly, et al. An image is worth 16x16 words: Transformers for image recognition at scale. *arXiv preprint arXiv:2010.11929*, 2020. 1, 2
- [19] Patrick Esser, Robin Rombach, and Bjorn Ommer. Taming transformers for high-resolution image synthesis. In *Proceedings of the IEEE/CVF conference on computer vision and pattern recognition*, pages 12873–12883, 2021. 2
- [20] Benjamin Graham, Alaaeldin El-Nouby, Hugo Touvron, Pierre Stock, Armand Joulin, Hervé Jégou, and Matthijs Douze. Levit: a vision transformer in convnet’s clothing for faster inference. In *Proceedings of the IEEE/CVF international conference on computer vision*, pages 12259–12269, 2021. 2, 3
- [21] Jianyuan Guo, Kai Han, Han Wu, Yehui Tang, Xinghao Chen, Yunhe Wang, and Chang Xu. Cmt: Convolutional neural networks meet vision transformers. In *Proceedings of the IEEE/CVF conference on computer vision and pattern recognition*, pages 12175–12185, 2022. 2
- [22] Meng-Hao Guo, Cheng-Ze Lu, Qibin Hou, Zhengning Liu, Ming-Ming Cheng, and Shi-Min Hu. Segnext: Rethinking convolutional attention design for semantic segmentation. *Advances in Neural Information Processing Systems*, 35:1140–1156, 2022. 6
- [23] Kai Han, Yunhe Wang, Qi Tian, Jianyuan Guo, Chunjing Xu, and Chang Xu. Ghostnet: More features from cheap

- operations. In *Proceedings of the IEEE/CVF conference on computer vision and pattern recognition*, pages 1580–1589, 2020. 2
- [24] Kaiming He and Georgia Gkioxari. P. Dollár, and Ross Girshick, “mask r-cnn,”. In *Proc. IEEE Int. Conf. Comput. Vis.*, pages 2980–2988, 2017. 1
- [25] Kaiming He, Xiangyu Zhang, Shaoqing Ren, and Jian Sun. Deep residual learning for image recognition. In *Proceedings of the IEEE conference on computer vision and pattern recognition*, pages 770–778, 2016. 1, 5, 6
- [26] Jonathan Ho, Nal Kalchbrenner, Dirk Weissenborn, and Tim Salimans. Axial attention in multidimensional transformers. *arXiv preprint arXiv:1912.12180*, 2019. 1
- [27] Andrew Howard, Mark Sandler, Grace Chu, Liang-Chieh Chen, Bo Chen, Mingxing Tan, Weijun Wang, Yukun Zhu, Ruoming Pang, Vijay Vasudevan, et al. Searching for mobilenetv3. In *Proceedings of the IEEE/CVF international conference on computer vision*, pages 1314–1324, 2019. 1, 2, 5, 6, 8
- [28] Andrew G Howard, Menglong Zhu, Bo Chen, Dmitry Kalenichenko, Weijun Wang, Tobias Weyand, Marco Andreetto, and Hartwig Adam. Mobilenets: Efficient convolutional neural networks for mobile vision applications. *arXiv preprint arXiv:1704.04861*, 2017. 1, 2, 4
- [29] Zilong Huang, Yousheng Ben, Guozhong Luo, Pei Cheng, Gang Yu, and Bin Fu. Shuffle transformer: Rethinking spatial shuffle for vision transformer. *arXiv preprint arXiv:2106.03650*, 2021. 4
- [30] Youngsaeng Jin, David Han, and Hanseok Ko. Trseg: Transformer for semantic segmentation. *Pattern Recognition Letters*, 148:29–35, 2021. 2
- [31] Beoungwoo Kang, Seunghun Moon, Yubin Cho, Hyunwoo Yu, and Suk-Ju Kang. Metaseg: Metaformer-based global contexts-aware network for efficient semantic segmentation. In *Proceedings of the IEEE/CVF Winter Conference on Applications of Computer Vision*, pages 434–443, 2024. 5, 6
- [32] Alexander Kirillov, Ross Girshick, Kaiming He, and Piotr Dollár. Panoptic feature pyramid networks. In *Proceedings of the IEEE/CVF conference on computer vision and pattern recognition*, pages 6399–6408, 2019. 5, 6
- [33] Hanchao Li, Pengfei Xiong, Haoqiang Fan, and Jian Sun. Dfanet: Deep feature aggregation for real-time semantic segmentation. In *Proceedings of the IEEE/CVF conference on computer vision and pattern recognition*, pages 9522–9531, 2019. 2
- [34] Jiachen Li, Ali Hassani, Steven Walton, and Humphrey Shi. Convmlp: Hierarchical convolutional mlps for vision. In *Proceedings of the IEEE/CVF Conference on Computer Vision and Pattern Recognition*, pages 6307–6316, 2023. 6
- [35] Xin Li, Yiming Zhou, Zheng Pan, and Jiashi Feng. Partial order pruning: for best speed/accuracy trade-off in neural architecture search. In *Proceedings of the IEEE/CVF Conference on Computer Vision and Pattern Recognition*, pages 9145–9153, 2019. 2
- [36] Yanyu Li, Geng Yuan, Yang Wen, Ju Hu, Georgios Evangelidis, Sergey Tulyakov, Yanzhi Wang, and Jian Ren. Efficientformer: Vision transformers at mobilenet speed. *Advances in Neural Information Processing Systems*, 35: 12934–12949, 2022. 1, 3
- [37] Yanyu Li, Ju Hu, Yang Wen, Georgios Evangelidis, Kamyar Salahi, Yanzhi Wang, Sergey Tulyakov, and Jian Ren. Rethinking vision transformers for mobilenet size and speed. In *Proceedings of the IEEE/CVF International Conference on Computer Vision*, pages 16889–16900, 2023. 1
- [38] Ze Liu, Yutong Lin, Yue Cao, Han Hu, Yixuan Wei, Zheng Zhang, Stephen Lin, and Baining Guo. Swin transformer: Hierarchical vision transformer using shifted windows. In *Proceedings of the IEEE/CVF international conference on computer vision*, pages 10012–10022, 2021. 3
- [39] Ze Liu, Han Hu, Yutong Lin, Zhuliang Yao, Zhenda Xie, Yixuan Wei, Jia Ning, Yue Cao, Zheng Zhang, Li Dong, et al. Swin transformer v2: Scaling up capacity and resolution. In *Proceedings of the IEEE/CVF conference on computer vision and pattern recognition*, pages 12009–12019, 2022. 1, 2
- [40] Jonathan Long, Evan Shelhamer, and Trevor Darrell. Fully convolutional networks for semantic segmentation. In *Proceedings of the IEEE conference on computer vision and pattern recognition*, pages 3431–3440, 2015. 6, 8
- [41] Ningning Ma, Xiangyu Zhang, Hai-Tao Zheng, and Jian Sun. Shufflenet v2: Practical guidelines for efficient cnn architecture design. In *Proceedings of the European conference on computer vision (ECCV)*, pages 116–131, 2018. 1, 2, 5, 6
- [42] Sachin Mehta and Mohammad Rastegari. Mobilevit: light-weight, general-purpose, and mobile-friendly vision transformer. *arXiv preprint arXiv:2110.02178*, 2021. 1, 2, 3
- [43] Sachin Mehta and Mohammad Rastegari. Separable self-attention for mobile vision transformers. *arXiv preprint arXiv:2206.02680*, 2022. 1
- [44] Sachin Mehta, Mohammad Rastegari, Linda Shapiro, and Hannaneh Hajishirzi. Espnetv2: A light-weight, power efficient, and general purpose convolutional neural network. In *Proceedings of the IEEE/CVF conference on computer vision and pattern recognition*, pages 9190–9200, 2019. 2
- [45] Yujian Mo, Yan Wu, Xinneng Yang, Feilin Liu, and Yujun Liao. Review the state-of-the-art technologies of semantic segmentation based on deep learning. *Neurocomputing*, 493: 626–646, 2022. 1
- [46] Roozbeh Mottaghi, Xianjie Chen, Xiaobai Liu, Nam-Gyu Cho, Seong-Whan Lee, Sanja Fidler, Raquel Urtasun, and Alan Yuille. The role of context for object detection and semantic segmentation in the wild. In *Proceedings of the IEEE conference on computer vision and pattern recognition*, pages 891–898, 2014. 2, 5, 8
- [47] Zhenliang Ni, Xinghao Chen, Yingjie Zhai, Yehui Tang, and Yunhe Wang. Context-guided spatial feature reconstruction for efficient semantic segmentation. *arXiv preprint arXiv:2405.06228*, 2024. 6
- [48] Junting Pan, Adrian Bulat, Fuwen Tan, Xiatian Zhu, Lukasz Dudziak, Hongsheng Li, Georgios Tzimiropoulos, and Brais Martinez. Edgevits: Competing light-weight cnns on mobile devices with vision transformers. In *European Conference on Computer Vision*, pages 294–311. Springer, 2022. 1, 3

- [49] Adam Paszke, Abhishek Chaurasia, Sangpil Kim, and Eugenio Culurciello. Enet: A deep neural network architecture for real-time semantic segmentation. *arXiv preprint arXiv:1606.02147*, 2016. 2, 8
- [50] Eduardo Romera, José M Alvarez, Luis M Bergasa, and Roberto Arroyo. Erfnet: Efficient residual factorized convnet for real-time semantic segmentation. *IEEE Transactions on Intelligent Transportation Systems*, 19(1):263–272, 2017. 2
- [51] Olaf Ronneberger, Philipp Fischer, and Thomas Brox. U-net: Convolutional networks for biomedical image segmentation. In *Medical image computing and computer-assisted intervention—MICCAI 2015: 18th international conference, Munich, Germany, October 5–9, 2015, proceedings, part III 18*, pages 234–241. Springer, 2015. 1
- [52] Mark Sandler, Andrew Howard, Menglong Zhu, Andrey Zhmoginov, and Liang-Chieh Chen. Mobilenetv2: Inverted residuals and linear bottlenecks. In *Proceedings of the IEEE conference on computer vision and pattern recognition*, pages 4510–4520, 2018. 1, 2, 3, 5, 6, 8
- [53] Wen Shi, Jing Xu, and Pan Gao. Ssformer: A lightweight transformer for semantic segmentation. *2022 IEEE 24th International Workshop on Multimedia Signal Processing (MMSP)*, pages 1–5, 2022. 1
- [54] Jae-hun Shim, Hyunwoo Yu, Kyeongbo Kong, and Suk-Ju Kang. Feedformer: Revisiting transformer decoder for efficient semantic segmentation. In *Proceedings of the AAAI Conference on Artificial Intelligence*, pages 2263–2271, 2023. 6
- [55] Ke Sun, Bin Xiao, Dong Liu, and Jingdong Wang. Deep high-resolution representation learning for human pose estimation. In *Proceedings of the IEEE/CVF conference on computer vision and pattern recognition*, pages 5693–5703, 2019. 5
- [56] Mingxing Tan and Quoc Le. Efficientnet: Rethinking model scaling for convolutional neural networks. In *International conference on machine learning*, pages 6105–6114. PMLR, 2019. 6, 8
- [57] Hugo Touvron, Matthieu Cord, Matthijs Douze, Francisco Massa, Alexandre Sablayrolles, and Hervé Jégou. Training data-efficient image transformers & distillation through attention. In *International conference on machine learning*, pages 10347–10357. PMLR, 2021. 2
- [58] Ao Wang, Hui Chen, Zijia Lin, Jungong Han, and Guiguang Ding. Repvit: Revisiting mobile cnn from vit perspective. In *Proceedings of the IEEE/CVF Conference on Computer Vision and Pattern Recognition*, pages 15909–15920, 2024. 6
- [59] Jingdong Wang, Ke Sun, Tianheng Cheng, Borui Jiang, Chaorui Deng, Yang Zhao, Dong Liu, Yadong Mu, Mingkui Tan, Xinggang Wang, et al. Deep high-resolution representation learning for visual recognition. *IEEE transactions on pattern analysis and machine intelligence*, 43(10):3349–3364, 2020. 6
- [60] Jian Wang, Chenhui Gou, Qiman Wu, Haocheng Feng, Junyu Han, Errui Ding, and Jingdong Wang. Rtfomer: Efficient design for real-time semantic segmentation with transformer. *Advances in Neural Information Processing Systems*, 35:7423–7436, 2022. 3
- [61] Libo Wang, Rui Li, Chenxi Duan, Ce Zhang, Xiaoliang Meng, and Shenghui Fang. A novel transformer based semantic segmentation scheme for fine-resolution remote sensing images. *IEEE Geoscience and Remote Sensing Letters*, 19:1–5, 2022. 2
- [62] Enze Xie, Wenhai Wang, Zhiding Yu, Anima Anandkumar, Jose M Alvarez, and Ping Luo. Segformer: Simple and efficient design for semantic segmentation with transformers. *Advances in neural information processing systems*, 34: 12077–12090, 2021. 1, 5, 6, 8
- [63] Seul-Ki Yeom and Julian von Klitzing. U-mixformer: Unet-like transformer with mix-attention for efficient semantic segmentation. *arXiv preprint arXiv:2312.06272*, 2023. 6
- [64] Changqian Yu, Jingbo Wang, Chao Peng, Changxin Gao, Gang Yu, and Nong Sang. Bisenet: Bilateral segmentation network for real-time semantic segmentation. In *Proceedings of the European conference on computer vision (ECCV)*, pages 325–341, 2018. 2
- [65] Kun Yuan, Shaopeng Guo, Ziwei Liu, Aojun Zhou, Fengwei Yu, and Wei Wu. Incorporating convolution designs into visual transformers. In *Proceedings of the IEEE/CVF international conference on computer vision*, pages 579–588, 2021. 4
- [66] Li Yuan, Yunpeng Chen, Tao Wang, Weihao Yu, Yujun Shi, Zi-Hang Jiang, Francis EH Tay, Jiashi Feng, and Shuicheng Yan. Tokens-to-token vit: Training vision transformers from scratch on imagenet. In *Proceedings of the IEEE/CVF international conference on computer vision*, pages 558–567, 2021. 3
- [67] Yuhui Yuan, Xilin Chen, and Jingdong Wang. Object-contextual representations for semantic segmentation. In *Computer Vision—ECCV 2020: 16th European Conference, Glasgow, UK, August 23–28, 2020, Proceedings, Part VI 16*, pages 173–190. Springer, 2020. 6
- [68] Ting Zhang, Guo-Jun Qi, Bin Xiao, and Jingdong Wang. Interleaved group convolutions. In *Proceedings of the IEEE international conference on computer vision*, pages 4373–4382, 2017. 2
- [69] Wenqiang Zhang, Zilong Huang, Guozhong Luo, Tao Chen, Xinggang Wang, Wenyu Liu, Gang Yu, and Chunhua Shen. Topformer: Token pyramid transformer for mobile semantic segmentation. In *Proceedings of the IEEE/CVF Conference on Computer Vision and Pattern Recognition*, pages 12083–12093, 2022. 1, 2, 3, 5, 6, 7, 8
- [70] Xiangyu Zhang, Xinyu Zhou, Mengxiao Lin, and Jian Sun. Shufflenet: An extremely efficient convolutional neural network for mobile devices. In *Proceedings of the IEEE conference on computer vision and pattern recognition*, pages 6848–6856, 2018. 1, 2
- [71] Hengshuang Zhao, Jianping Shi, Xiaojuan Qi, Xiaogang Wang, and Jiaya Jia. Pyramid scene parsing network. In *Proceedings of the IEEE conference on computer vision and pattern recognition*, pages 2881–2890, 2017. 6, 8
- [72] Hengshuang Zhao, Xiaojuan Qi, Xiaoyong Shen, Jianping Shi, and Jiaya Jia. Icnnet for real-time semantic segmentation on high-resolution images. In *Proceedings of the European conference on computer vision (ECCV)*, pages 405–420, 2018. 2

- [73] Bolei Zhou, Hang Zhao, Xavier Puig, Sanja Fidler, Adela Barriuso, and Antonio Torralba. Scene parsing through ade20k dataset. In *Proceedings of the IEEE conference on computer vision and pattern recognition*, pages 633–641, 2017. [2](#), [5](#), [6](#), [7](#)
- [74] Daquan Zhou, Qibin Hou, Yunpeng Chen, Jiashi Feng, and Shuicheng Yan. Rethinking bottleneck structure for efficient mobile network design. In *Computer Vision–ECCV 2020: 16th European Conference, Glasgow, UK, August 23–28, 2020, Proceedings, Part III 16*, pages 680–697. Springer, 2020. [2](#)
- [75] Lei Zhu, Xinjiang Wang, Zhanghan Ke, Wayne Zhang, and Rynson WH Lau. Biformer: Vision transformer with bi-level routing attention. In *Proceedings of the IEEE/CVF conference on computer vision and pattern recognition*, pages 10323–10333, 2023. [2](#)



# ContextFormer: Redefining Efficiency in Semantic Segmentation

## Supplementary Material

Mian Muhammad Naeem Abid, Nancy Mehta, Zongwei Wu, Fayaz Ali Dharejo, Radu Timofte  
Computer Vision Lab, CAIDAS, University of Würzburg, Germany

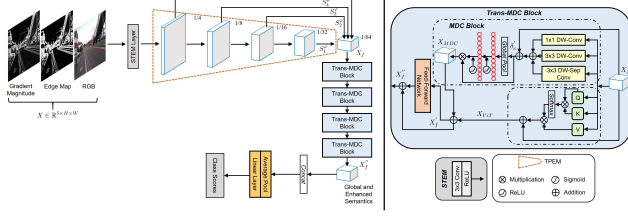


Figure 4. The architecture of the proposed ContextFormer model for the task of image classification.

In this supplementary, we illustrate the ImageNet pre-training and results for the task of image classification (Sec. 6), model architecture with details (Sec. 7), design of Feed-Forward Network (Sec. 8), visual results (Sec. 9), and limitations with future work (Sec. 10).

### 6. ImageNet Pre-training

For a fair comparison, we initialize the ContextFormer model using pre-trained parameters from ImageNet. As demonstrated in Fig. 4, the classification framework of ContextFormer integrates an average pooling layer followed by a linear layer, leveraging global semantic representations to generate class scores. Given the low resolution of the input images ( $224 \times 224$ ), the target resolution of the input tokens for the Trans-MDC block is configured to be  $\frac{1}{64} \times \frac{1}{64}$  of the input dimensions. Quantitative results of the proposed ContextFormer model on the ImageNet-1K dataset are shown in Tab. 7.

Table 7. ContextFormer results for ImageNet classification.

Method	Input Size	Top-1 Accuracy(%)	GFLOPs	Parameters
ContextFormer	$224 \times 224$	66.1	0.13	1.79M
ContextFormer <sub>(GME)</sub>	$224 \times 224$	66.4	0.13	1.79M

### 7. Detailed Network Structure

The detailed network structure of the proposed ContextFormer model for the efficient real-time semantic segmentation task is provided in Tab. 8. Where,  $dw$  and  $dw.sep$  denote depth-wise and depth-wise separable convolutions. Moreover,  $N$ ,  $H$  and  $T$  denote the number of blocks, number of heads and number of target channels, respectively. The input image resolution taken into account is  $512 \times 512$ .

Table 8. Architectural details of ContextFormer model. For input resolution of  $512 \times 512$ .

Stage	Details					Output Resolution
	layer	kernel size	expand ratio	output channels	stride	
Stem	Conv	3	-	16	2	$256 \times 256$
	MobileNetV2	3	1	16	1	
TPEM	MobileNetV2	3	4	16	2	$128 \times 128$
	MobileNetV2	3	3	16	1	
	MobileNetV2	5	3	32	2	$64 \times 64$
	MobileNetV2	5	3	32	1	
	MobileNetV2	3	3	64	2	$32 \times 32$
	MobileNetV2	3	3	64	1	
MDC Block	MobileNetV2	5	6	96	2	$16 \times 16$
	MobileNetV2	5	6	96	1	
	Trans-MDC Block					
ViT Block	$3 \times 3_{dw}$	3	-	208	1	$8 \times 8$
	$1 \times 1_{dw}$	1	-	208	1	
	$3 \times 3_{dw.sep}$	3, 1	-	208	1	
	N=4					
	N=4, H=4					$8 \times 8$
FMM	T=160					$8^2, 16^2, 32^2, 64^2$
GFLOPs	-					0.6

### 8. Details of Feed-Forward Network

In the proposed ContextFormer model, the unified output semantics from the MDC block and ViT block are passed through the Feed-Forward Network. For the Feed-Forward Network, we have integrated depth-wise convolution layer between  $1 \times 1$  convolution layers and to further minimize the computational complexity, expansion factor of two is incorporated which helps the Trans-MDC block to augment the capturing of global semantics. The design of Feed-Forward Network is shown in Fig. 5.

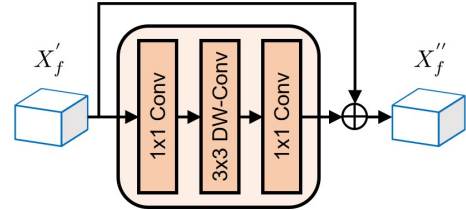


Figure 5. Design of Feed-Forward Network.

### 9. Visual Results

Fig. 6 shows additional visual results of the proposed ContextFormer model with original images, ground-truth, TopFormer, and ContextFormer<sub>(GME)</sub>. The proposed model demonstrates superior segmentation performance on the validation set of the ADE20K benchmark dataset, highlighting its robustness.

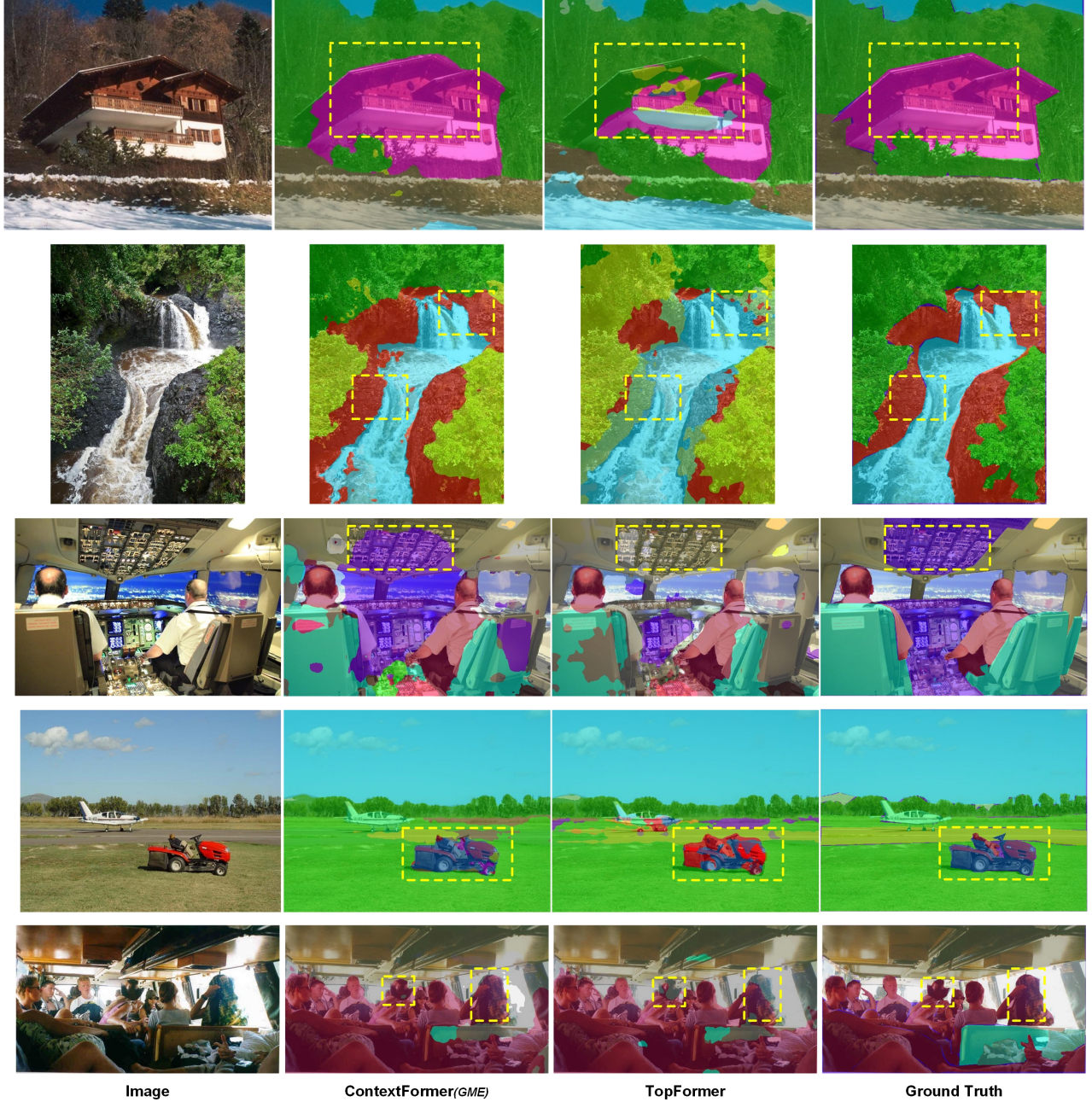


Figure 6. Visual results on the ADE20K validation set. Our proposed model illustrates superior consistency with the ground truth segmentation results, highlighting its robustness.

## 10. Limitations and Future Work

The proposed model exhibits strong performance and efficiency in semantic segmentation tasks. However, certain limitations warrant further investigation. A notable constraint for lightweight efficient models, including ours, is their dependency on pre-training with the ImageNet-1K dataset to achieve optimal performance; the absence of such

pre-training leads to a significant decline in effectiveness. Future work will focus on improving the model’s robustness and efficiency across diverse datasets and practical scenarios. Expanding the scope of testing and validation will be crucial to establish the model’s generalizability. Furthermore, emphasis will be placed on adapting and refining the model for real-world applications to enhance its practical utility.